J|A|C|S COMMUNICATIONS

Published on Web 11/12/2010

Biologically Inspired Highly Durable Iron Phthalocyanine Catalysts for Oxygen Reduction Reaction in Polymer Electrolyte Membrane Fuel Cells

Wenmu Li, Aiping Yu, Drew C. Higgins, Bernard G. Llanos, and Zhongwei Chen*

Department of Chemical Engineering, Waterloo Institute for Nanotechnology, Waterloo Institute for Sustainable Energy, University of Waterloo, 200 University Avenue West, Waterloo, Ontario, Canada N2L 3G1

Received July 13, 2010; E-mail: zhwchen@cape.uwaterloo.ca

Abstract: In the present work, we have designed and synthesized a new highly durable iron phtalocyanine based nonprecious oxygen reduction reaction (ORR) catalyst (Fe-SPc) for polymer electrolyte membrane fuel cells (PEMFCs). The Fe-SPc, with a novel structure inspired by that of naturally occurring oxygen activation catalysts, is prepared by a nonpyrolyzing method, allowing adequate control of the atomic structure and surface properties of the material. Significantly improved ORR stability of the Fe-SPc is observed compared with the commercial Fe-Pc catalysts. The Fe-SPc has similar activity to that of the commercial Fe-Pc initially, while the Fe-SPc displays 4.6 times higher current density than that of the commercial Fe-Pc after 10 sweep potential cycles, and a current density that is 7.4 times higher after 100 cycles. This has been attributed to the incorporation of electron-donating functional groups, along with a high degree of steric hindrance maintaining active site isolation. Nonprecious Fe-SPc is promising as a potential alternative ORR electrocatalyst for PEMFCs.

Polymer electrolyte membrane (PEM) fuel cells are regarded as ideal candidates for stationary and mobile power generation due to their high energy conversion efficiency and low environmental impacts.[1] A key obstacle to widely commercializing PEM fuel cells is the high cost of component materials, specifically the platinum based electrocatalysts to mediate reactions at the electrodes. Improvements in the utilization and activity of platinum (Pt) catalysts have served to reduce the platinum loading. However, steadily increasing costs and dwindling supplies of Pt have offset this progress in reducing the cost of fuel cell systems. Thus, various types of nonprecious oxygen reduction reaction (ORR) catalyst materials have been investigated to replace platinum including nitrides,[2] chalcogenides,[3,4] nitrogen-doped carbon nanotubes,[5] metal-doped conductive polymers,[6] and metal-N_4 chelates macrocycles.[7] Significant progress has been made with respect to iron based catalysts, which is generally considered a leading candidate.[8] However, traditional experiments have utilized iron based catalysts subjected to high temperature pyrolysis during synthesis, making it extremely difficult to tailor the structure and surface properties. This has resulted in trial and error based experiments aimed at optimizing the ORR activity by manipulating synthesis conditions, with the actual nature of the active sites a subject of debate. Nonpyrolyzed iron based catalysts on the other hand have attracted interest because they provide the ability to adequately control the structure and surface properties of the materials.

Iron phthalocyanine (Fe-Pc, Figure 1A) and iron porphyrine (Fe-PPY) complexes can endure acidic aqueous conditions. However, when exposed to harsh PEM fuel cell oxygen reducing environments, even these relatively stable macrocycle compounds will degrade due to demetalation. Demetalation can occur either by degradation of the macrocycle structure,[7b,c] resulting in the loss of Fe, or due to the replacement of Fe^{2+} ions by protons present in the system.[7f] Regardless, it has been shown that these phenomena are a consequence of slow electron transfer properties and close packing of the macrocycle compounds (Figure 1C, distance between neighbor Fe−Fe is 4.119 Å).[7b,f] Naturally occurring oxygen activation catalysts, which have been utilized in biological processes for billions of years, provide a fundamental basis for overcoming these durability issues.[9] First, the addition of electron-donating functional groups (Cu and phenol groups) serves to prevent the formation and release of detrimental partially reduced oxygen byproducts and intermediates.[10] Second, bulky protein chains are utilized to provide a large degree of separation between ORR active sites, preventing site overlap and catalytic deactivation.[11]

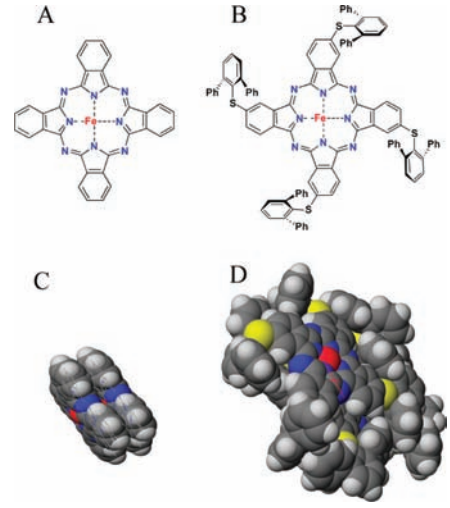

Figure 1. Atomic structure of (A) Fe-Pc and (B) Fe-SPc and the space filling stacking model of (C) Fe-Pc (d_{Fe-Fe}: 4.119 Å) and (D) Fe-SPc (d_{Fe-Fe}: 6.945 Å); side view, same scale.

This has formed the basis for the present work in which we have carefully designed and synthesized a novel Fe-Pc based catalyst material [Ferrous 2,9,16,23-tetra-(2′,6′-diphenylphenthioether)phthalocyanine, Fe-SPc], with a structure inspired by that of naturally occurring oxygen activation catalysts (Figure 1B, Scheme S1). Thioether functional groups are attached to phthalocyanine macrocycles to act as supplementary electron-providing sites to prevent issues arising from slow electron transfer. Furthermore, bulky diphenyl thiophenol groups are incorporated into the structure providing a high degree of steric hindrance, maintaining isolation between catalytically active sites (Figure 1D, distance between neighbor Fe−Fe is 6.945 Å).

Fourier transfer infrared (FTIR), nuclear magnetic resonance (NMR), and high resolution electron spray ionization mass spectroscopy (ESI-MS) were used to confirm the formation and purity

10.1021/ja106217u

of the final products (Figures S1 and S2 in the Supporting Information (SI)). ESI-MS performed on Fe(II)-SPc mainly shows two strong peak distributions. One is centered at $m/2z = 804.71$ (Figures 2 and S3), which could be assigned to Fe(III)-SPc cation free radical species **A** (Figure S3A). The other is centered at $m/2z = 1609.45$ which could be assigned to Fe(III) μ-oxo dimers cation free radicals **C** (Figure S3C).[12] The isotopic distribution of this envelope of peaks is consistent with iron. It is interesting that most of Fe(II)-SPc loses two electrons and converts into Fe(III)-SPc cation free radicals, whereas only a small amount of Fe(II)-SPc turns into Fe(III)-SPc **B** (Figure S3B), a result of losing one electron through ESI-MS characterization. The initial transfer of two electrons to oxygen molecules is imperative to ORR with respect to oxygen trapping and activation.[13] ESI-MS characterization indicated that Fe-SPc readily loses two electrons, suggesting that this compound may favor oxygen trapping in the early stages. This hypothesis is confirmed as oxygen trapped $[Fe(III)\text{-}SPc]_2\text{-}O_2$ cation free radicals **D** (Figure S3D) were detected in the ESI-MS.

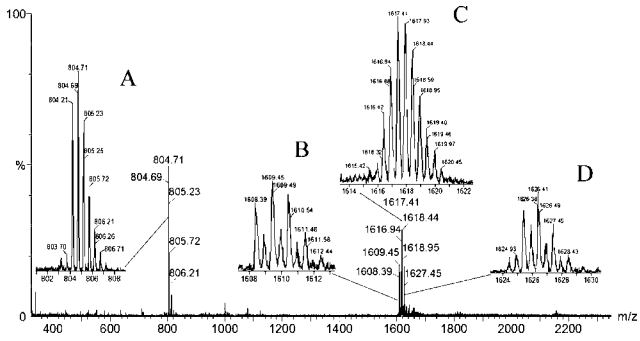

Figure 2. ESI-MS distribution of Fe-SPc, showing peaks attributed to (A) Fe(III)-SPc cation free radical, (B) Fe(III)-SPc, (C) Fe(III)-SPc μ-oxo dimers cation free radicals, and (D) $[Fe(III)\text{-}SPc]_2\text{-}O_2$ cation free radicals.

This investigation involves the first design and synthesis of Fe-SPc materials as ORR electrocatalysts; thus it would be of great importance to isolate the exact site of ORR on these compounds. We have opted to utilize cyanide (CN^-) as an inhibitor molecule, as CN^- is known to be the strongest single ligand. The CN^- ions bind with a high affinity to many oxidized Fe(III) hemeproteins but possess a minimal affinity to reduced Fe(II) species.[14] Assuming that $Fe(II)CN^-\text{−}Pc$ compounds display similar stability as $Fe(II)CN^-\text{−}$heme complexes, the following proposition is made. We propose that complete blockage of the Fe(II) active sites present in Fe−Pc complexes by CN^- ions was impossible and O_2 binding would be preferential (Reaction 1, Scheme S2). Once the $Fe(II)\text{−}O_2$ complex is formed, a single electron transfer from Fe(II) to O_2 occurs immediately, forming $Fe(III)\text{−}O_2^{\bullet -}$ (Reaction 1 in Scheme S2). Due to the high affinity of CN^- ions to the Fe(III) metal center, the adsorbed superoxide molecule ($O_2^{\bullet -}$) will immediately be replaced by CN^- ions (Reaction 3, Scheme S2). The release of the superoxide molecule will result in the formation of HO_2^- species following the transfer of a single electron (overall two-electron reduction) from the electrode surface in an alkaline solution (Reaction 4 Scheme S2). Yeager et al. carried out an investigation on Fe-TsPc, where a shift from a four-electron to a two-electron ORR was observed in the presence of 1 mM KCN.[15] This shift to a two-electron ORR in the presence of CN^- ions aligns well with our proposed mechanism to identify the iron center as the active site for the ORR. In order to verify this proposition with Fe-SPc, ORR analysis was carried out in the presence of CN^- ions (from KCN). A shift from a four-electron to two-electron ORR was observed, accompanied by a shift in half wave potential (Figure S4A). This confirms that the ORR active site of Fe-SPc is the iron ion center.

The stability of the Fe-SPc catalyst supported on KJ300 (Fe-SPc/KJ300) was investigated by continuously applying linear potential sweeps from 0 to 1.2 V vs RHE using a rotating ring disk electrode (RRDE) setup. The ORR polarization curves obtained before and after 100 potential sweeps displayed a 14.5% decrease in current density at a potential of 0.5 V vs RHE (Figure 3A, Table S1). In contrast, the degradation of Fe-Pc/KJ300 was very rapid with a 89.1% decrease in current density at 0.5 V vs RHE after just 100 cycles (Figure 3B, Table S1). The improved stability is apparent after just 10 cycles from looking at Figure 3. After just 10 cycles, the current density at an electrode potential of 0.5 V vs RHE is 4.6 times higher for Fe-SPc, compared with Fe-Pc. Furthermore, after 100 cycles the current density observed is 7.4 times higher. There are two well accepted mechanisms for the deactivation of Fe-Pc catalysts: either (i) degradation of the Fe-Pc structure by ORR intermediates[7b,c] or (ii) demetalation of the phthalocyanine as previously discussed.[7f] Fe-SPc on the other hand does display some cycle dependent activity losses. These can be attributed to either degradation of the active sites or oxidation of the carbon support material.[16] However, future work must be directed at elucidating these possibilities.

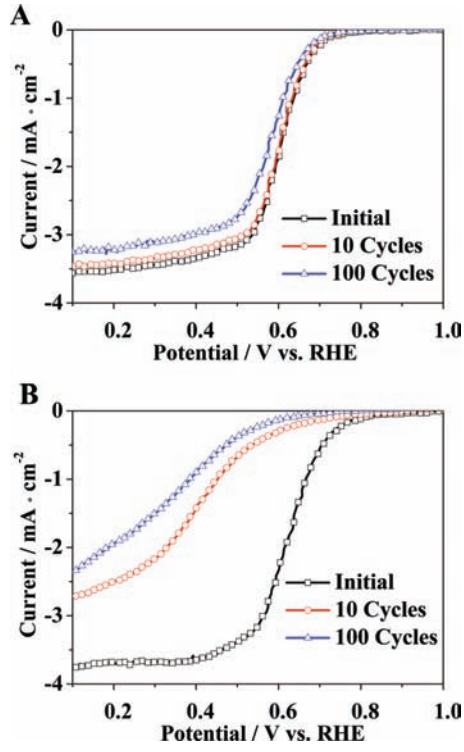

Figure 3. Polarization curves for the ORR on (A) Fe-SPc/KJ300 and (B) Fe-Pc/KJ300 catalysts on an RRDE, displaying initial activity along with activity observed after 10 and 100 potential sweeps in oxygen saturated electrolyte. Curves were obtained at a sweep rate of 10 mV/s and an electrode rotation speed of 400 rpm.

Insight into the ORR and degradation mechanisms on these iron based catalysts will be provided, coupled with background information obtained from previous studies. Some researchers believe that the demetalation degradation occurs due to the decrease in diameter of the iron center from Fe(II) (1.56 Å) to Fe(III) (1.29 Å).[7f,17] However, in another experiment, at high potentials (above 0.77 V vs RHE), it was reported that all iron should be in the form of

Fe(III).[7d] Other reports have indicated the stability of Fe(III)-Pc is quite good in inert (nitrogen or argon saturated) acidic conditions.[7b] To verify this, we have tested the stability of Fe-SPc by continuous linear potential sweeps in nitrogen saturated 0.1 M $HClO_4$. The stability of Fe-SPc is excellent, with only a 8.3% decrease in current density at an electrode potential of 0.5 V vs RHE after 1200 potential cycles (Figure S5). In the presence of oxygen, however, it has been reported that slow electron transfer coupled with free protons in solution could speed up the degradation of Fe-Pc molecules.[7b,f] These previous observations indicate the importance of investigating the iron catalyzed ORR mechanistic pathway in order to further elucidate and understand the behavior of these nonprecious catalysts in the presence of oxygen. The consensus is that the iron activated ORR mechanism begins with the Fe(II) site, because of the low binding energy of Fe(II)$-H_2O$ (0.10 eV), which makes water molecules readily replaceable by dioxygen [Fe(II)$-O_2$ (0.12 eV)].[18] As this binding occurs, either two electrons are transferred from the iron compound or one electron is transferred from the iron compound and the other from the electrode, resulting in the formation of Fe(III)OO^-.[13a] Transfer of another electron, coupled with the addition of a single proton, results in the formation of an Fe(II)O$-$OH complex. Mixed reports arose regarding the subsequent breaking of the protonated ferrous Fe(II)O$-$OH bond. One specific report suggested that a second proton could facilitate the heterolytic scission of Fe(II)O$-$OH to form transient Fe(IV)-oxo intermediates and water.[13b] The highly valent Fe(IV)-oxo molecules have been well documented as intermediates of heme or nonheme iron catalysts for ORR.[19] The diameter of Fe(IV) is around 1.17 Å which is significantly smaller than that of Fe(III) in a high spin state (1.29 Å).[17] If the electron transfer is quick from the electrode to the Fe(IV)-oxo to reduce it to Fe(III), problems will not arise. However, hindered electron transfer will prolong the lifetime of Fe(IV)-oxo, increasing the probability of replacing the Fe(IV) ion by protons from the phthalocyanine macrocycle. Furthermore, the Fe(IV)-oxo is notorious for its high oxidation activity toward most organic compounds.[20] Thus, it is expected that it could also catalyze the degradation of neighboring Fe-Pc molecules and carbon supports. This could answer the question why Fe-Pc is stable under an inert atmosphere, whereas, in the presence of oxygen, the demetalation of Fe-Pc is facilitated. On the contrary, Fe-SPc contains supplementary electron-donating groups to alleviate the problem of slow electron transfer, temporarily supplying electrons to reduce the Fe(IV)-oxo compound before any degradation effects occur. The presence of $m/2z = 804.71$ (Figure 2A) in the ESI-MS spectrum of Fe-SPc indirectly confirms that supplementary electrons are readily donated from the thiol functionalized macrocycle.

Figure S7 compares the ORR activity for Fe-SPc and commercially available Fe-Pc monomers supported on KJ-300 using RRDE techniques. The Fe-SPc/KJ300 displays a half wave potential that is 20 mV lower than that of Fe-Pc/KJ300. In addition, for both samples, the ring currents show negligible H_2O_2 generation, indicating a four-electron reduction of O_2 to H_2O (more detailed analyses, including Koutecky$-$Levich (Figure S8B) and number of electrons transferred (Figure S8C), are available in the SI). Furthermore, the tolerance of the cathode catalysts to methanol was characterized by linear potential sweeps of commercial Pt/C and Fe-SPc catalysts in 0.1 M $HClO_4$, both with and without methanol. The results indicate that the methanol oxidation current densities on the Fe-SPc catalysts are negligible compared to that on the Pt/C catalyst (Figure S8D). This indicates that these catalysts are more tolerant to methanol crossover compared with Pt/C and could also be used as a methanol tolerant cathode catalyst in direct methanol fuel cells.

This study demonstrates the feasibility of developing novel iron phthalocyanine ORR catalysts that offer high stability under fuel cell conditions. Comparing the electrochemical properties of Fe-SPc catalysts with those of Fe-Pc also serves to elucidate the mechanisms involved in the iron activated ORR mechanism. Fe-SPc catalysts are presented as potential nonprecious ORR catalyst alternatives, with a carefully designed structure inspired by that of naturally occurring oxygen activation catalysts.

Acknowledgment. This work was financially supported by the Natural Sciences and Engineering Research Council of Canada (NSERC) and the University of Waterloo. We thank Dr. Allan S Hay at McGill University for his kind help.

Supporting Information Available: Additional figures, references, and experimental procedures. This material is available free of charge via the Internet at http://pubs.acs.org.

References

(1) Vielstich, W.; Lamm, A.; Gasteiger, H. A. *Handbook of fuel cells: fundamentals, technology, and applications*; Wiley: Chichester, U.K.; Hoboken, NJ, 2003.
(2) Zhong, H. X.; Zhang, H. M.; Liu, G.; Liang, Y. M.; Hu, J. W.; Yi, B. L. *Electrochem. Commun.* **2006**, *8*, 707.
(3) Vayner, E.; Sidik, R. A.; Anderson, A. B.; Popov, B. N. *J. Phys. Chem. C* **2007**, *111*, 10508.
(4) Feng, Y. J.; He, T.; Alonso-Vante, N. *Chem. Mater.* **2008**, *20*, 26.
(5) (a) Sidik, R. A.; Anderson, A. B.; Subramanian, N. P.; Kumaraguru, S. P.; Popov, B. N. *J. Phys. Chem. B* **2006**, *110*, 1787. (b) Tang, Y. F.; Allen, B. L.; Kauffman, D. R.; Star, A. *J. Am. Chem. Soc.* **2009**, *131*, 13200. (c) Liu, G.; Li, X. G.; Ganesan, P.; Popov, B. N. *Appl. Catal., B* **2009**, *93*, 156.
(6) (a) Bashyam, R.; Zelenay, P. *Nature* **2006**, *443*, 63. (b) Yuan, X. X.; Zeng, X.; Zhang, H. J.; Ma, Z. F.; Wang, C. Y. *J. Am. Chem. Soc.* **2010**, *132*, 1754. (c) Olson, T. S.; Pylypenko, S.; Atanassov, P.; Asazawa, K.; Yamada, K.; Tanaka, H. *J. Phys. Chem. C* **2010**, *114*, 5049.
(7) (a) Jasinski, R. *Nature* **1964**, *201*, 1212. (b) Meier, H.; Tschirwitz, U.; Zimmerhackl, E.; Albrecht, W.; Zeitler, G. *J. Phys. Chem.* **1977**, *81*, 712. (c) Tanaka, A. A.; Fierro, C.; Scherson, D.; Yeager, E. B. *J. Phys. Chem.* **1987**, *91*, 3799. (d) Vanderputten, A.; Elzing, A.; Visscher, W.; Barendrecht, E. *J. Electroanal. Chem.* **1987**, *221*, 95. (e) Zagal, J. H. *Coord. Chem. Rev.* **1992**, *119*, 89. (f) Baranton, S.; Coutanceau, C.; Roux, C.; Hahn, F.; Leger, J. M. *J. Electroanal. Chem.* **2005**, *577*, 223. (g) Baker, R.; Wilkinson, D. P.; Zhang, J. J. *Electrochim. Acta* **2009**, *54*, 3098. (h) Harnisch, F.; Wirth, S.; Schroder, U. *Electrochem. Commun.* **2009**, *11*, 2253. (i) Jahnke, H.; Schonborn, M.; Zirnmermann, G. *Physical and chemical applications of dyestuffs*; Springer-Verlag: Berlin; New York, 1976; p 135.
(8) (a) Jaouen, F.; Herranz, J.; Lefevre, M.; Dodelet, J. P.; Kramm, U. I.; Herrmann, I.; Bogdanoff, P.; Maruyama, J.; Nagaoka, T.; Garsuch, A.; Dahn, J. R.; Olson, T.; Pylypenko, S.; Atanassov, P.; Ustinov, E. A. *ACS Appl. Mater. Interfaces* **2009**, *1*, 1623. (b) Lefevre, M.; Proietti, E.; Jaouen, F.; Dodelet, J. P. *Science* **2009**, *324*, 71.
(9) Zagal, J. H.; Bedioui, F.; Dodelet, J.-P. *N_4-macrocyclic metal complexes*; Springer: New York, 2006.
(10) (a) Proshlyakov, D. A.; Pressler, M. A.; DeMaso, C.; Leykam, J. F.; DeWitt, D. L.; Babcock, G. T. *Science* **2000**, *290*, 1588. (b) Collman, J. P.; Devaraj, N. K.; Decreau, R. A.; Yang, Y.; Yan, Y. L.; Ebina, W.; Eberspacher, T. A.; Chidsey, C. E. D. *Science* **2007**, *315*, 1565.
(11) Shirai, H.; Higaki, S.; Hanabusa, K.; Kondo, Y.; Hojo, N. *J. Polym. Sci., Polym. Chem.* **1984**, *22*, 1309.
(12) Ercolani, C.; Gardini, M.; Murray, K. S.; Pennesi, G.; Rossi, G. *Inorg. Chem.* **1986**, *25*, 3972.
(13) (a) Babcock, G. T.; Wikstrom, M. *Nature* **1992**, *356*, 301. (b) Harris, D. L.; Loew, G. H. *J. Am. Chem. Soc.* **1998**, *120*, 8941.
(14) (a) Yoshikawa, S.; Okeeffe, D. H.; Caughey, W. S. *J. Biol. Chem.* **1985**, *260*, 3518. (b) Li, J. F.; Lord, R. L.; Noll, B. C.; Baik, M.-H.; Schulz, C. E.; Robert Scheidt, W. R. *Angew. Chem., Int. Ed.* **2008**, *47*, 10144.
(15) Gupta, S.; Fierro, C.; Yeager, E. *J. Electroanal. Chem.* **1991**, *306*, 239.
(16) (a) Borup, R.; et al. *Chem. Rev.* **2007**, *107*, 3904. (b) Huang, S. Y.; Ganesan, P.; Park, S.; Popov, B. N. *J. Am. Chem. Soc.* **2009**, *131*, 13898.
(17) Shannon, R. D. *Acta Crystallogr., Sect. A* **1976**, *32*, 751.
(18) Anderson, A. B.; Sidik, R. A. *J. Phys. Chem. B* **2004**, *108*, 5031.
(19) Li, F. F.; England, J.; Que, L. *J. Am. Chem. Soc.* **2010**, *132*, 2134.
(20) (a) Perollier, C.; Pergrale-Mejean, C.; Sorokin, A. B. *New J. Chem.* **2005**, *29*, 1400. (b) Que, L.; Tolman, W. B. *Nature* **2008**, *455*, 333.

JA106217U